Original article

Variability of Available Potential Energy Density and Buoyancy Work in the Upper 300-m Layer of the Black Sea Based on the Simulation Results

S. G. Demyshev, O. A. Dymova ✉, N. A. Miklashevskaya

Marine Hydrophysical Institute of RAS, Sevastopol, Russian Federation
✉ *olgadym@yahoo.com*

Abstract
Purpose. The study is aimed at identifying possible physical mechanisms for the variability of available potential energy density and buoyancy fluxes in the upper active layer of the Black Sea.
Methods and Results. Spatial distribution of the available potential energy density and buoyancy fluxes was studied based on analyzing the thermohaline characteristics of the Black Sea circulation in 2011 and 2016 resulted from the numerical experiments performed using the Black Sea dynamics model developed in the Marine Hydrophysical Institute. The model included the EMODNet bathymetry and the SKIRON system data on wind velocity, heat fluxes, precipitation, evaporation, and sea surface temperature. The numerical experiments provided the daily fields of current velocities, temperature and salinity based on which the density of available potential energy and the buoyancy work were calculated. It is shown that the spatial-temporal variability of the available potential energy density in the Black Sea was formed by the mechanisms different for the upper 30-m layer and for the main halocline layer. The buoyancy work was revealed to be of seasonal variability.
Conclusions. In the upper layer, the variability of the available potential energy density is related primarily to the propagation of freshened river waters, whereas in the main halocline layer (75–150 m), the field structure is conditioned by mesoscale dynamics. In the first case, the increased values of the available potential energy density are observed during a year on the northwestern shelf and on the basin periphery; in the central part of the sea, the distribution of available potential energy density is determined by the atmospheric conditions. In the layer below 75 m, the maximum values of the available potential energy density correspond to the anticyclonic eddies. In consequence of the intensive water mixing in the upper active layer during the cold period of a year, the buoyancy work is conditioned by vertical velocity. In a spring-summer period, a two-layer structure of the field is observed which governed by the sign of density anomalies. The upper layer thickness constitutes 20–30 m and corresponds to the depth of seasonal thermocline. In the main halocline, the highest absolute values of the buoyancy work are observed in the zones of intense mesoscale anticyclones.

Keywords: Black Sea, numerical modeling, eddies, available potential energy, buoyancy work, current velocities, seasonal variability

Acknowledgments: Numerical experiments and analysis of thermohaline characteristics were performed by O. A. Dymova with the financial support of the RSF grant No. 22-77-10056. The analysis of energy characteristics was carried out within the framework of the state task on topic No. FNNN-2021-0004 (code "Oceanological processes").

For citation: Demyshev, S.G., Dymova, O.A. and Miklashevskaya, N.A., 2023. Variability of Available Potential Energy Density and Buoyancy Work in the Upper 300-m Layer of the Black Sea Based on the Simulation Results. *Physical Oceanography*, 30(3), pp. 355-368. doi:10.29039/0233-7584-2023-3- 355-368

DOI: 10.29039/1573-160X-2023-3- 355-368

Introduction

Available potential energy (APE) is one of the key concepts in the analysis of mechanical energy transformation in the atmosphere and ocean. By definition, APE

is a part of the total potential energy that can be converted into kinetic energy (KE). The main physical processes that form the APE budget are energy dissipation and buoyancy work when moving water masses in the vertical direction. Buoyancy fluxes at the region boundaries (free surface, river mouths and straits) can both be sources and sinks of APE. According to classical concepts [1–3], the APE release in the ocean and its transformation into KE is associated with eddy variability. Modern researchers confirm this concept based on the results of realistic numerical experiments and observational data [4–6]. In addition to the APE estimates as the main source of energy for mesoscale eddies in the ocean, the APE dissipation plays an important role in turbulent mixing [7, 8]. The contribution of the ocean APE to the global ocean – atmosphere interaction is discussed in [9]. It follows from the foregoing that the analysis of the mechanisms of APE variability is an urgent problem in oceanology.

For the Black Sea, the APE reserve estimates based on observational data are presented, for example, in the monograph [1] and in the works [10, 11]. According to the authors, the average APE density in the upper active layer is about 20–30 J/m^3; it was also indicated in [10, 11] that the highest APE density is observed in the permanent halocline layer (75–150 m). There are few works on the numerical analysis of the APE budget in the Black Sea. The first quantitative estimates of the buoyancy work contribution can be found in [12]. In [13], for the first time for the Black Sea, a method for numerical analysis of all components of the energy budget was proposed and the results for climate circulation were presented. Energy transitions between the APE and KE in an idealized (circulation is driven by a stationary wind) two-layer model were studied in [14].

According to the results of numerical experiments with realistic atmospheric conditions [15–17], it was demonstrated that the average annual integral energy flux formed by the buoyancy work is directed from the average APE to the mean current KE. Consequently, the mean circulation in the Black Sea is supported by both wind pumping and baroclinic instability of the mean current. In the case of a weakened wind action, the energy contributions of the buoyancy fluxes can be commensurate with the contribution of the wind work (see Fig. 6, in [17, p. 268]).

An analysis of seasonal variability of energy characteristics [18] revealed that the value of the APE density significantly depends on the season of the year: its highest values are observed in summer and are located in the layer from the surface to the upper boundary of the seasonal thermocline (upper 20 m layer). The vertical distribution of the buoyancy work is more complex and irregular. In the upper 20 m layer, the buoyancy work is positive, which indicates the transformation of energy from the APE to the KE; in the 20–40 m layer, it is negative, i.e. the APE increases due to the KE. Positive values predominate below.

The purpose of this work is to study in detail the spatial distribution of the APE density and buoyancy fluxes based on the analysis of the thermohaline circulation characteristics and to identify possible physical mechanisms for the variability of the APE and buoyancy fluxes in the upper active layer of the Black Sea.

[1] Blatov, A.S., Bulgakov, N.P., Ivanov, V.A., Kosarev, A.N. and Tuljulkin, V.S., 1984. *Variability of the Black Sea Hydrophysical Fields*. Leningrad: Gidrometeoizdat, 240 p. (in Russian).

Materials and methods

This work is a continuation of the study begun in [17, 18], therefore, to achieve the set goal, the results of two numerical experiments on modeling the Black Sea circulation in 2011 and 2016 were used. These years were chosen based on the considerations that the water dynamics reflected the "basin" (2011) and "eddy" (2016) circulation regimes [19]. In the first case, the structure of the current field was dominated by the Rim Current, in the second case, mesoscale eddies dominated in the central part.

The calculations were performed using the model of the Marine Hydrophysical Institute (MHI) [20]. The model is based on the complete system of ocean thermohydrodynamic equations in the Boussinesq approximation, hydrostatics, and seawater incompressibility. The density nonlinearly depends on temperature and salinity. Level height is calculated using a linearized free surface kinematic condition. Heat fluxes, precipitation, evaporation, and tangential wind stress are set as boundary fields on the sea surface. At the bottom, no-slip conditions and absence of heat and salt fluxes are set, bottom friction is not taken into account. On the solid side sections of the boundary, the free-slip conditions are satisfied, and the normal derivatives are set equal to zero for temperature and salinity. On the liquid sections of the boundary, the river inflow and water exchange through the straits are taken into account. Vertical turbulent mixing is parameterized using the Mellor – Yamada turbulent closure model. Horizontal turbulent viscosity and diffusion are represented by biharmonic operators with a coefficient of 10^{16} $cm^4 \cdot s^{-1}$.

The MHI model is implemented on the *C* grid with a uniform step along the horizontal coordinates of 1.6 km, 27 uneven *z*-horizons are specified vertically with a concentration in the upper active layer. The bathymetry of the basin was built according to EMODnet data (available at: http://portal.emodnet-bathymetry.eu) with (1/8)′ resolution. As an atmospheric forcing, 6-hour data on wind velocity at 10 m height, evaporation, sea surface temperature, heat and precipitation fluxes provided by the SKIRON system with a spatial resolution of 0.1° [21] were used. The mathematical formulation of the MHI model, the parameters of numerical experiments, and the validation of the calculation results are presented in detail in [17]. In general, the structure of the model circulation corresponds to the generally accepted concepts for the Black Sea [22]: in the autumn-winter season, there is an increase in the current velocity and intense vertical mixing; in the warm season – weakening of the basin dynamics, development of mesoscale eddies of various signs, heating and freshening of the upper layers of the sea, formation of a cold intermediate layer.

As a result of numerical experiments, we obtained daily fields of current velocity, temperature, and salinity, from which the APE and the buoyancy work were calculated. The main hydrophysical fields for evaluating the studied energy characteristics are the density of seawater and the vertical component of the current velocity. In the MHI model, the local density ρ is calculated using the Mamaev formula [23] as a nonlinear dependence on temperature and salinity:

$$\rho = \rho_0\left(1 + \alpha_1^T T + \alpha_1^S S + \alpha_2^T T^2 + \alpha^{TS} TS\right),$$

where ρ_0 is a fresh water density; *T* is temperature; *S* is salinity; α are coefficients of thermal expansion and salinity contraction [23].

Vertical velocity is calculated from the continuity equation

$$w = -\int_0^z \left(\frac{\partial u}{\partial x} + \frac{\partial v}{\partial y}\right) dz,$$

where u, v are horizontal components of velocity vectors; w is vertical velocity. The MHI model is built in the right Cartesian coordinate system: the x-axis is directed to the east, the y-axis – to the north, and the z-axis – down from the surface to the bottom. A positive or negative vertical velocity value determines the downwelling or upwelling, respectively. The accuracy of the continuity equation is 10^{-12} cm/s.

For the ocean, there is no exact formula for the APE calculation, so we used the formula proposed in [24]:

$$P_m = \frac{1}{2}\int_V \frac{g}{n_0(z)}\overline{\rho^*}^2\, dV, \qquad n_0(z) = \frac{d\langle\rho\rangle}{dz}, \qquad \rho^* = \rho - \langle\rho\rangle, \tag{1}$$

where P_m is a mean APE; V is a layer volume; g is a gravitational acceleration; ρ is local density; ρ* is a local density anomaly. The bar above the symbol denotes time averaging; < > is averaging over the layer area, taking into account the "land – sea" mask. The parameter ⟨ρ⟩ is calculated as the local density averaged over the corresponding model horizon and is a constant for each layer. In formula (1), in contrast to the formula applied in [24], there is no minus sign before the integral. This is due to the choice of z axis direction (down in the MHI model), which leads to positive values of the vertical density gradient, which coincides with the direction of gravity. The buoyancy work BW is calculated by the formula

$$BW = \int_V g\overline{\rho^*}\overline{w}\, dV. \tag{2}$$

Formula (2) is strictly derived from the equations of the KE and APE variation rate. As demonstrated in [3, 12, 13, 16], the buoyancy work enters both equations as a separate term, only its sign in the corresponding equation differs. Consequently, the magnitude and sign of the buoyancy work indicate the intensity and direction of energy conversion between the KE and APE. In the MHI model, a positive value of BW corresponds to the transformation from APE to KE. The time averaging interval in formulas (1) and (2) is chosen to be one month, which makes it possible to take into account seasonal variations in energy fluxes.

Results

For the analysis, the average monthly values of the APE density and the buoyancy work density for each model horizon were calculated and the fields T, S, w, ρ*, P_m and BW were compared at 5, 30, 50, and 100 m horizons, as well as vertical sections of all indicated characteristics on the zonal section along 43°N. Further in the text, for brevity, we omit the term "density" to denote the APE and the buoyancy work per unit volume.

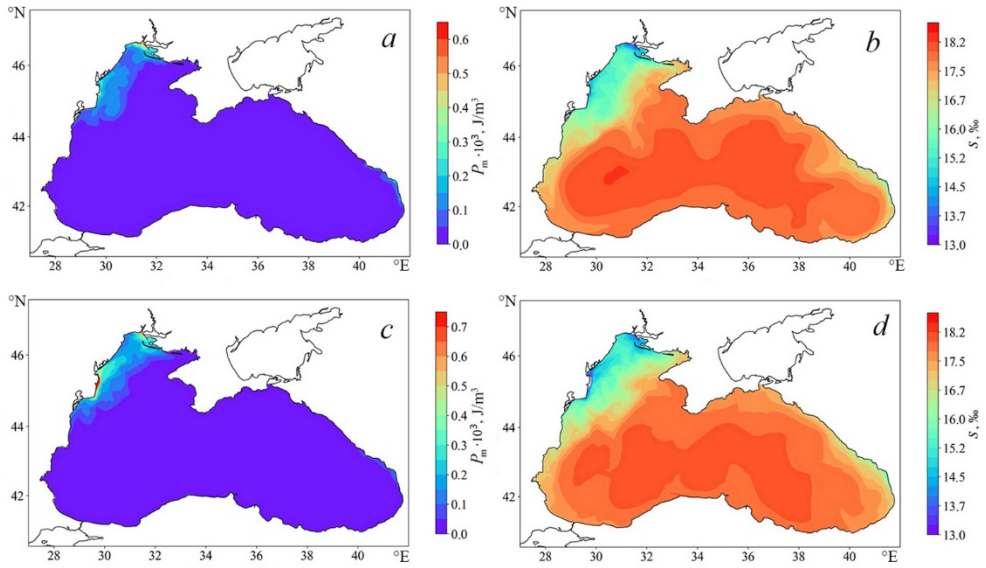

F i g. 1. Monthly average APE density (*a*, *c*) and salinity (*b*, *d*) at the 5 m horizon in July 2011 (*a*, *b*) and July 2016 (*c*, *d*)

For both considered periods, the spatial structures of the APE fields, salinity, and density anomaly at all horizons are qualitatively similar. The zones of the maximum APE values coincide with the localization of low salinity values. In the upper 20-meter layer, the APE spatiotemporal variability reflects the influence of river runoff and atmospheric conditions. Throughout the year, the highest APE values are observed in the area of the mouths of the Dnieper and Danube rivers; in the central part of the sea, APE changes insignificantly. In Fig. 1, the average fields of APE and salinity for July at 5 m horizon in 2011 and 2016 are demonstrated. It can be seen that the highest APE values in the northwestern part of the sea are related to the zones of coastal water freshening (Fig. 1, *b*, *d*), which are formed due to river runoff.

As the depth increases, the APE decreases by 1–2 orders of magnitude. At the horizons below 50 m, the APE spatial structure is determined by eddy activity. In Fig. 2 the distributions of APE and salinity at 100 m horizon in 2011 and 2016 are given. The areas of increased APE values (Fig. 2, *a*, *c*) coincide with the zones of large density anomalies in absolute value, which are formed as a result of salinity variations (Fig. 2, *b*, *d*) during the upwelling and downwelling in cyclonic and anticyclonic eddies, respectively. Let us note that the APE store in anticyclones (areas of low salinity in Fig. 2, *b*, *c*) is higher than in cyclones, approximately 2–3 times.

The seasonal variability of atmospheric fluxes has little effect on the APE in the main halocline layer. For the periods under study, the maximum APE at a horizon of 100 m was found in July 2011 in the Batumi anticyclone zone, and in March and October 2016 in the Sevastopol anticyclone zone.

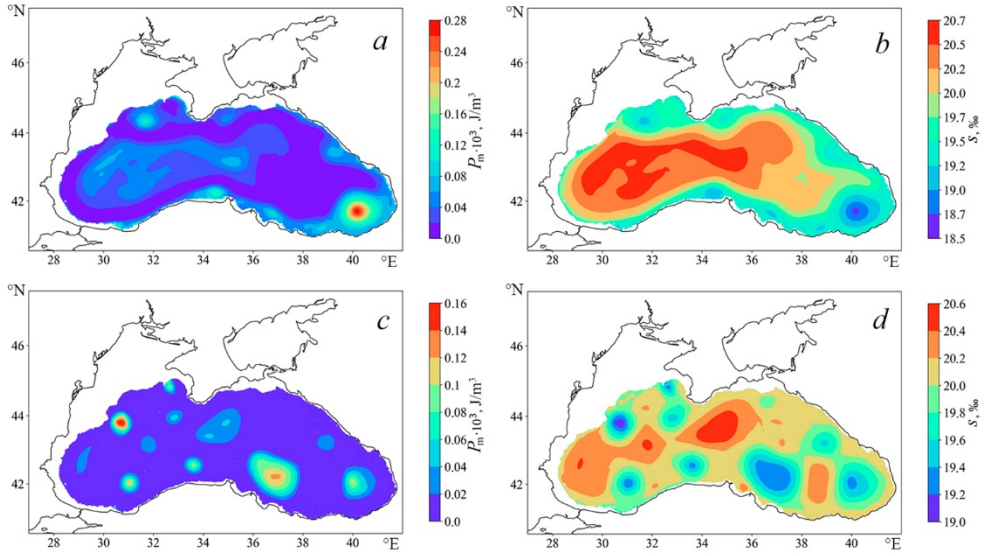

F i g. 2. Monthly average APE density (*a*, *c*) and salinity (*b*, *d*) at the 100 m horizon in June 2011 (*a*, *b*) and June 2016 (*c*, *d*)

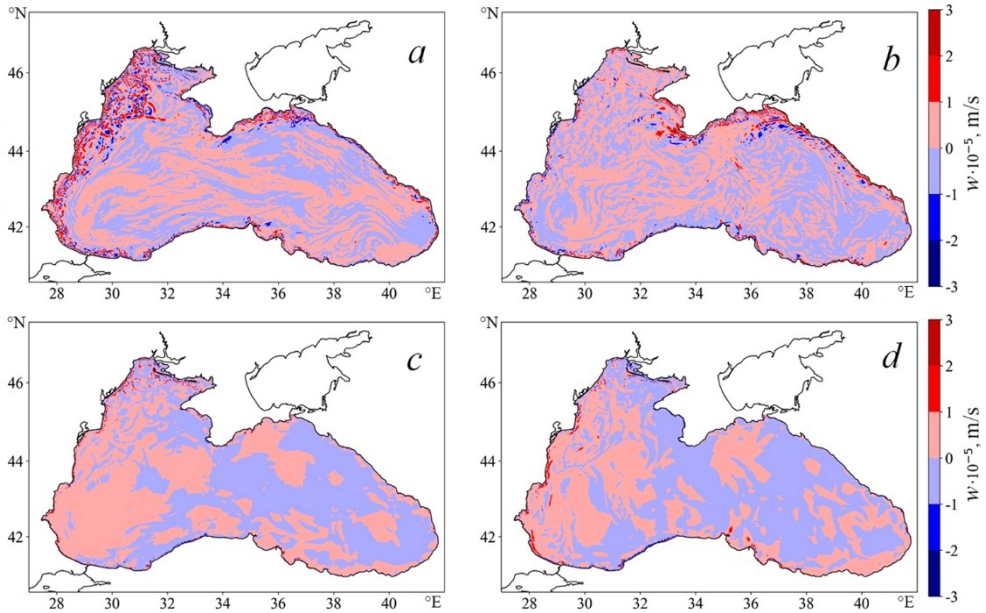

F i g. 3. Vertical velocity averaged over the upper 30 m layer in February 2011 (*a*), February 2016 (*b*), August 2011 (*c*), and August 2016 (*d*)

According to the results of the analysis, the spatiotemporal variability of the buoyancy work can be conventionally divided into two types: in the upper 30-m layer and in the layer of the main halocline (50–150 m according to [22]). We are to consider in more detail the causes for such a distribution in depth. In the upper layer for both periods, the density anomalies are positive in the cold season and negative

in the warm season. Therefore, the spatial distribution of the *BW* value positive and negative areas is determined only by the change in the vertical velocity sign. As can be seen from Fig. 3, *a*, *b*, in autumn and winter, the vertical velocity (and, consequently, the buoyancy work field) is characterized by a strong alternation of zones of positive and negative values with maximum absolute values at the basin periphery. In June – September (Fig. 3, *c*, *d*) in the eastern part of the sea, the areas of upwelling ($w < 0$) prevail, in the western part – the areas of downwelling ($w > 0$). Thus, in summer, in the upper layer of the western part of the sea, energy is converted from KE to APE ($BW < 0$), and vice versa in the eastern part, from APE to KE ($BW > 0$), regardless of the circulation regime.

Below 30 m horizon, there is no horizontal uniformity of density anomalies in space. This is primarily due to the basin cyclonic circulation pattern of the Black Sea waters (Fig. 4, *a*), which causes the lowering of isopycnals at the basin periphery and rise in the central part, thus forming a positive density anomaly in the center (Fig. 4, *c*). At a weak cyclonic circulation (Fig. 4, *b*), the lowering of the isopycnals near the continental slope is weakly expressed.

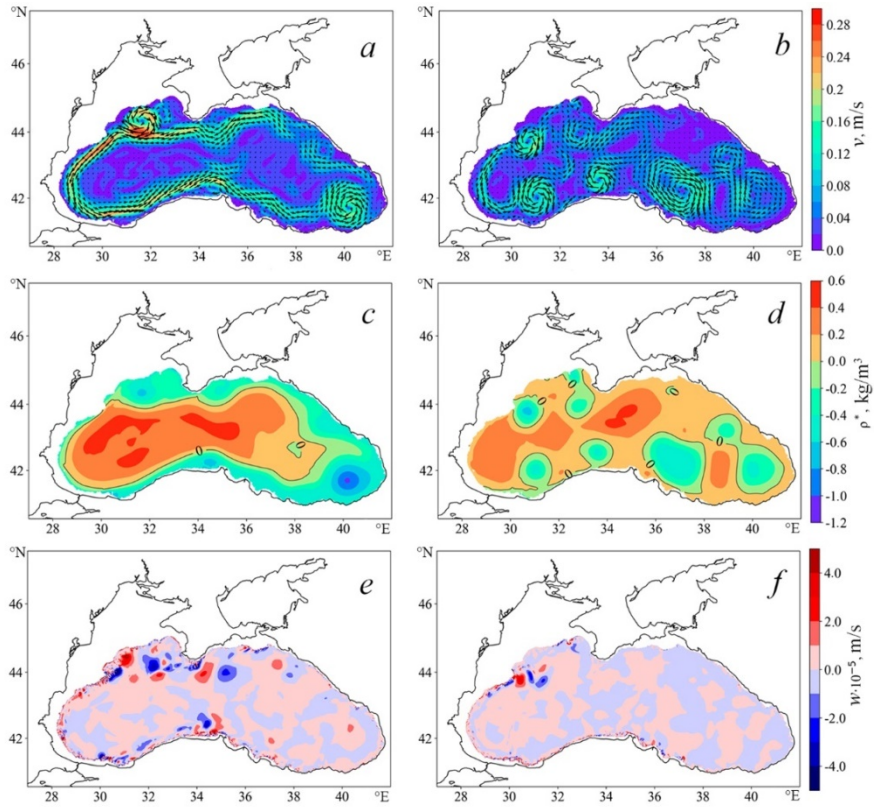

F i g. 4. Monthly average horizontal (*a*, *b*) and vertical (*e*, *f*) velocities, and density anomaly (*c*, *d*) at the 100 m horizon in June 2011 (*a*, *c*, *e*) and June 2016 (*b*, *d*, *f*)

However, in both experiments, intense mesoscale anticyclones developing near the slope (Fig. 4, *a*, *b*) contribute to the additional inflow of desalinated water from

overlying horizons, which clearly manifests itself in the form of areas with minimum values of density anomalies (Fig. 4, *c*, *d*) and maximum values of vertical velocity (Fig. 4, *e*, *f*).

At the same time, upwelling at the periphery of anticyclones, which can be demonstrated by the example of the Sevastopol anticyclone. In Fig. 5, the distribution of horizontal (Fig. 5, *a*) and vertical (Fig. 5, *b*) velocities in the Sevastopol anticyclone in mid-June 2011 is given. It can be seen that in the core of the eddy (approximately the area with coordinates 44.23°N, 31.5°E), the waters fall ($w > 0$) and isohalines are deflected. At the eddy periphery, the waters rise (gradation of blue in Fig. 5, *b*), and the rise rate is higher at the right boundary, where increased values of the orbital velocity are observed. In cyclonic eddies the situation is reversed: in the center the water rises, at the periphery it falls. As can be seen from Fig. 5, *c*, the core of the cyclonic eddy in the southeastern part of the sea in June 2016 corresponds to the rise of isohalines (Fig. 5, *d*).

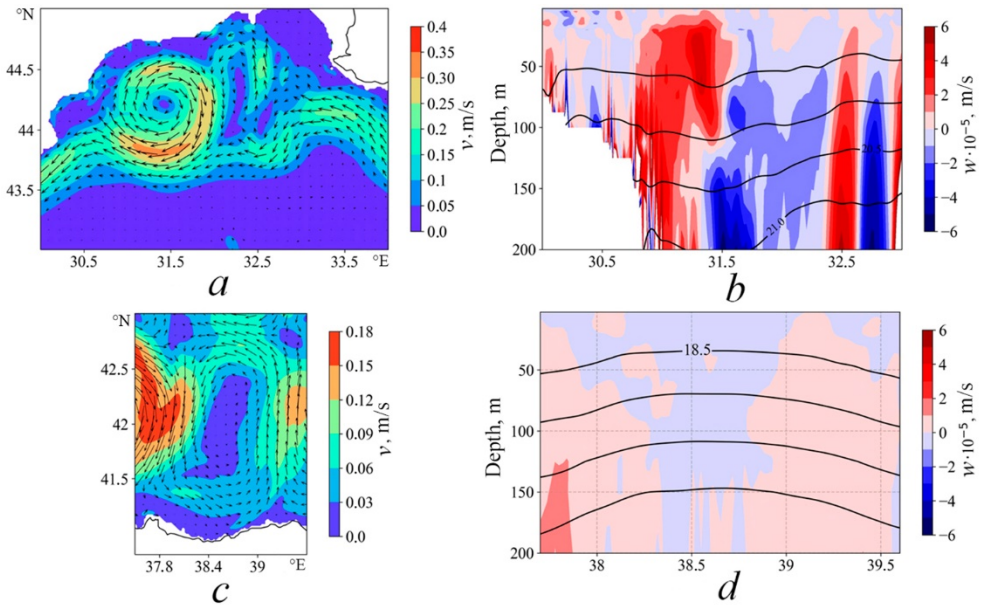

F i g. 5. Horizontal velocity at the 100 m horizon (*a*, *c*), vertical velocity on the zonal sections along 44.23°N (*b*) and 42°N (*d*) on June 15, 2011 (*a*, *b*) and June 18, 2016 (*c*, *d*). Black lines denote isohalines (shading is 0.5‰)

Positive and negative density anomalies and alternation of the zones of upwelling and downwelling lead to a complex structure of the buoyancy work field below the 30 m horizon. In Fig. 6, the average *BW* maps for June for two calculations are demonstrated. By virtue of the form of formula (2), the zero isolines of *BW*, ρ*, and *w* coincide. Along the isoline separating positive and negative density anomalies (Fig. 4, *c*, *d*), a change in the sign of the buoyancy work (Fig. 6, *a*, *b*) for both experiments is observed. This boundary spatially corresponds to the Rim Current

core in 2011 (Fig. 4, *a*) and the areas of mesoscale eddy formations in 2016 (Fig. 4, *b*). The minimum *BW* values are observed in the cores of anticyclonic eddies with maximum orbital and vertical velocities, the *BW* maxima are observed at the periphery of intense anticyclones. In the central deep part of the sea, the range of *BW* variability is several times smaller than in eddies, and the change in the vertical velocity sign may be due to fast dynamic and thermohaline processes, which are difficult to identify on the average monthly maps of the studied parameters. Thus, the most energy-active zones in terms of energy conversion between kinetic and available potential energy are mesoscale anticyclones.

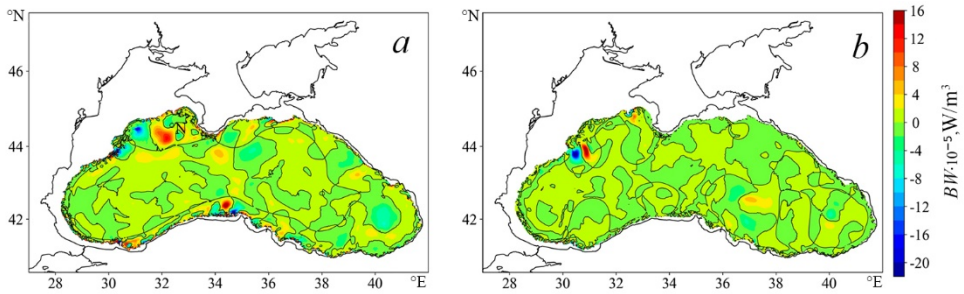

F i g. 6. Monthly average buoyancy work per unit volume at the 100 m horizon in June 2011 (*a*) and June 2016 (*b*)

The analysis of vertical sections of energy and hydrophysical fields in 2011 and 2016 revealed that the maximum APE values are localized in the coastal northwestern part of the sea, where river waters are distributed (Fig. 1, *a*, *c*). Vertically, the river runoff effect can be traced down to 25–30 m depths. The APE density decreases with depth, and areas of increased values are observed in the spatial distribution (compared to the surrounding waters), which can be identified as a manifestation of eddy activity in the halocline layer. In Fig. 7, the zonal sections of the APE and salinity fields are demonstrated. It can be seen that in the 75–125 m layer in the central part of the sea the increased APE values correspond to the zones of change in the isohaline slopes. As shown in Fig. 5, the isohaline deflection corresponds to the downwelling in the anticyclone core, the rise corresponds to the upwelling in the cyclone core. Thus, by analogy, we can conclude that the largest APE values in the area of isohaline descent (indicated by the red arrow in Fig. 7, *b*) are in the anticyclone, and the largest APE values in the area of isohaline rise (blue arrows in Fig. 7, *a*) are in the cyclone. The obtained result is confirmed by the fact that anticyclones in the Black Sea are more intense [25]. This conclusion is consistent with Fig. 2, *c*, where the increased APE values on the 100 m horizon spatially correspond to the zones with the maximum and minimum density anomalies (Fig. 4, *d*) in the cyclones and anticyclones (Fig. 4, *b*), respectively. It should be noted that the temporal variability of the APE in the upper layer of the coastal zone is determined by the seasonal increase in river runoff, while

no relationship with the change of seasons was found in the halocline layer. The APE maxima below the 30 m horizon were detected in April 2011 (Fig. 7, *a*) and in November 2016 (Fig. 7, *b*).

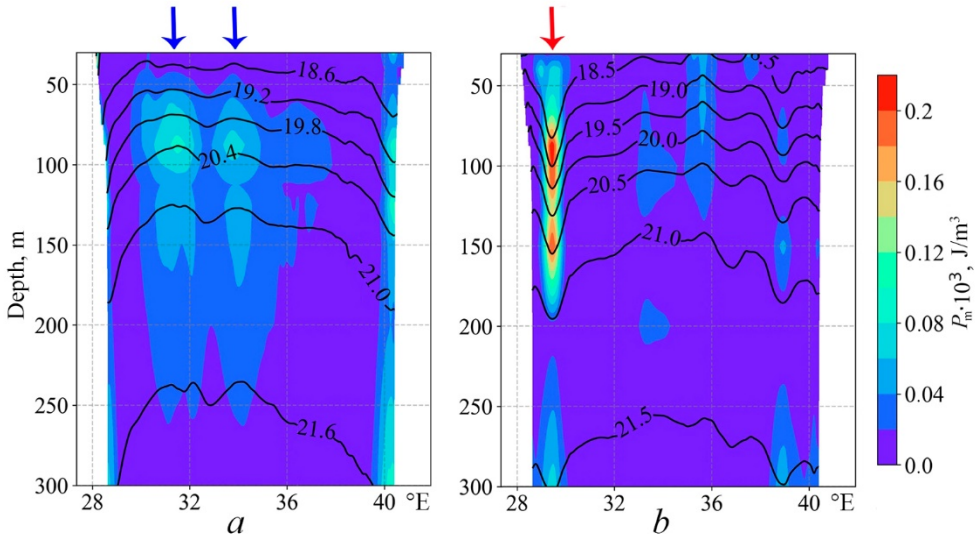

F i g. 7. Monthly average APE density (color) and salinity (black lines) on the zonal section along 43° N in April 2011 (*a*) and November 2016 (*b*)

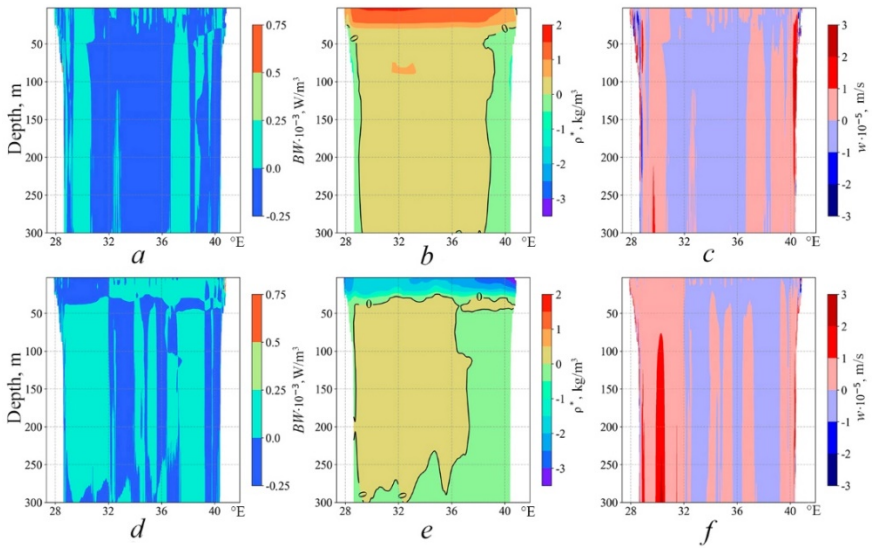

F i g. 8. Monthly average buoyancy work per unit volume (*a*, *d*), density anomaly (*b*, *e*) and vertical velocity (*c*, *f*) on the zonal section along 43° N in March (*a* – *c*) and August (*d* – *f*), 2011

According to formula (2), the sign of the buoyancy work depends on the product of vertical velocity and density anomaly. In Fig. 8, the vertical sections of *BW*, ρ* and *w* at the end of the winter and summer hydrological seasons are given. In the

cold season, when the density anomaly is sufficiently uniform along the vertical (Fig. 8, *b*), the direction of energy conversion between the APE and the KE is determined by the zones of upwelling and downwelling. Where the water rises ($w < 0$, blue color gradation in Fig. 8, *c*), the buoyancy work is negative, therefore, the APE increases due to the KE. In the warm season, when the density anomaly changes sign with depth (Fig. 8, *e*), the buoyancy work (Fig. 8, *d*) also changes sign depending on the ones of ρ* and *w*. In Fig. 8, *d*, a certain nominal boundary approximately at 30 m depth, crossing which the buoyancy work changes sign, is observed. The 20–30 m layer for these experiments corresponds to the depth of the seasonal thermocline (Fig. 10 in [18, p. 15]). Thus, in the warm period, when the structure of the density anomaly field changes due to the formation of a seasonal thermocline, the buoyancy work can change sign with depth. At the same time, in the vertical velocity distribution, no relationship with the depth of the seasonal thermocline or the depth of the permanent halocline was found. Qualitatively, this situation was repeated in 2016 with the difference that there were more *BW* and *w* regions of different signs due to the intense eddy circulation variability in 2016 compared to 2011.

Conclusion

According to the results of the experiments, the spatial and temporal variability of the APE density in the Black Sea is formed by various mechanisms for the upper 30-meter layer and the layer of the main halocline. In the upper layer, the APE variability is associated primarily with the distribution of freshened river waters. Thus, during the year, the maximum values of the APE density are observed in the area of the northwestern shelf, and increased values are observed at the basin periphery. The upper layer in the central part of the sea is subject to weak spatial and temporal variability, and the APE density here is determined by atmospheric conditions.

In the 75–150 m layer of the main halocline, the structure of the APE density field is determined by the mesoscale dynamics. The APE density maximum values correspond to the zones of negative density anomalies that are formed in anticyclonic eddies. An analysis of the APE density horizontal spatial distribution revealed that the most energy-active zones of the Black Sea are the areas of the Sevastopol and Batumi anticyclones, and when the orbital velocity of the eddy is bigger, then the APE is higher. It is noted that the APE density in cyclones is 2–3 times less than in anticyclones. Such a structure corresponds to the fact that the anticyclones in the Black Sea are more intense and, therefore, the isopycnal slopes in them are steeper, which leads to an increase in density anomalies.

The buoyancy work variability, which determines the rate and direction of energy transformation between the APE and KE, manifests a seasonal character. In the cold period, due to intense mixing, positive density anomaly is formed in the entire upper active layer of the Black Sea. Therefore, the buoyancy work is largely determined by the vertical velocity sign. In the central part, where the water rises, the energy flux is directed from the KE to the APE, and vice versa at the periphery of the basin. In spring and summer, in the buoyancy work field, a two-

layer structure determined by zones of positive and negative density anomalies is observed. The thickness of the upper layer is 20–30 m and, according to our work published in *Water* journal in 2022, corresponds to the seasonal thermocline depth.

An analysis of the structure of buoyancy work field in the main halocline showed that the most intense energy conversion between the APE and KE occurs in the zones of mesoscale anticyclonic eddies with maximum orbital velocities. Moreover, the buoyancy work sign is determined mainly by the vertical velocity sign, which is multidirectional in the core and at the periphery of the eddy.

REFERENCES

1. Kamenkovich, V.M., Koshlyakov, M.N. and Monin, A.S., eds., 1986. *Synoptic Eddies in the Ocean*. Dordrecht: Springer, 444 p. doi:10.1007/978-94-009-4502-9
2. Gill, A.E., 1982. *Atmosphere – Ocean Dynamics*. San Diego, USA: Academic Press, 662 p. doi:10.1016/s0074-6142(08)x6002-4
3. Holland, W.R., 1975. Energetics of Baroclinic Oceans. In: NAS, 1975. *Numerical Models of Ocean Circulation: Proceedings of a Symposium Held at Durham, New Hampshire, October 17-20, 1972*. Washington: National Academy of Sciences, pp. 168-177.
4. Luecke, C.A., Arbic, B.K., Bassette, S.L., Richman, J.G., Shriver, J.F., Alford, M.H., Smedstad, O.M., Timko, P.G., Trossman, D.S. and Wallcraft, A.J., 2017. The Global Mesoscale Eddy Available Potential Energy Field in Models and Observations. *Journal of Geophysical Research: Oceans*, 122(11), pp. 9126-9143. doi:10.1002/2017JC013136
5. Li, Q., Zhou, L. and Xie, L., 2021. Seasonal and Interannual Variability of EAPE in the South China Sea Derived from ECCO2 Data from 1997 to 2019. *Water*, 13(7), 926. doi:10.3390/w13070926
6. Travkin, V.S. and Belonenko, T.V., 2021. Study of the Mechanisms of Vortex Variability in the Lofoten Basin Based on Energy Analysis. *Physical Oceanography*, 28(3), pp. 294-308. doi:10.22449/1573-160X-2021-3-294-308
7. Winters, K.B., Lombard, P.N., Riley, J.J. and D'Asaro, E.A., 1995. Available Potential Energy and Mixing in Density-Stratified Fluids. *Journal of Fluid Mechanics*, 289, pp. 115-128. doi:10.1017/S002211209500125X
8. Tailleux, R., 2013. Irreversible Compressible Work and Available Potential Energy Dissipation in Turbulent Stratified Fluid. *Physica Scripta*, 2013(T155), 014033. doi:10.1088/0031-8949/2013/T155/014033
9. Bishop, S.P., Small, R.J. and Bryan, F.O., 2020. The Global Sink of Available Potential Energy by Mesoscale Air-Sea Interaction. *Journal of Advances in Modeling Earth Systems*, 12(10), e2020MS002118. doi:10.1029/2020MS002118
10. Simonov, A.I. and Altman, E.N., eds., 1991. *Hydrometeorology and Hydrochemistry of Seas in the USSR. Vol. IV. Black Sea. Issue 1. Hydrometeorological Conditions*. Saint Petersburg: Gidrometeoizdat, 428 p. (in Russian).
11. Suvorov, A.M. and Shokurova, I.G., 2004. Annual and Interdecadal Variability of the Available Potential Energy in the Black Sea. *Physical Oceanography*, 14(2), pp. 84-95. doi:10.1023/B:POCE.0000037872.25674.ac
12. Stanev, E.V., 1990. On the Mechanisms of the Black Sea Circulation. *Earth-Science Reviews*, 28(4), pp. 285-319. doi:10.1016/0012-8252(90)90052-W

13. Demyshev, S.G., 2004. Energy of the Black Sea Climatic Circulation. Part I: Discrete Equations of the Time Rate of Change of Kinetic and Potential Energy. *Meteorologiya i Gidrologiya*, (9), pp. 65-80 (in Russian).

14. Pavlushin, A.A., Shapiro, N.B. and Mikhailova, E.N., 2019. Energy Transitions in the Two-Layer Eddy-Resolving Model of the Black Sea. *Physical Oceanography*, 26(3), pp. 185-201. doi:10.22449/1573-160X-2019-3-185-201

15. Demyshev, S.G. and Dymova, O.A., 2013. Numerical Analysis of the Mesoscale Features of Circulation in the Black Sea Coastal Zone. *Izvestiya, Atmospheric and Oceanic Physics*, 49(6), pp. 603-610. doi:10.1134/S0001433813060030

16. Demyshev, S.G. and Dymova, O.A., 2018. Numerical Analysis of the Black Sea Currents and Mesoscale Eddies in 2006 and 2011. *Ocean Dynamics*, 68(10), pp. 1335-1352. doi:10.1007/s10236-018-1200-6

17. Demyshev, S.G. and Dymova, O.A., 2022. Analysis of the Annual Mean Energy Cycle of the Black Sea Circulation for the Climatic, Basin-Scale and Eddy Regimes. *Ocean Dynamics*, 72(3-4), pp. 259-278. doi:10.1007/s10236-022-01504-0

18. Demyshev, S., Dymova, O. and Miklashevskaya, N., 2022. Seasonal Variability of the Dynamics and Energy Transport in the Black Sea by Simulation Data. *Water*, 14(3), 338. doi:10.3390/w14030338

19. Stanev, E.V. and Staneva, J.V., 2000. The Impact of the Baroclinic Eddies and Basin Oscillations on the Transitions between Different Quasi-Stable States of the Black Sea Circulation. *Journal of Marine Systems*, 24(1-2), pp. 3-26. doi:10.1016/S0924-7963(99)00076-7

20. Demyshev, S.G., 2012. A Numerical Model of Online Forecasting Black Sea Currents. *Izvestiya, Atmospheric and Oceanic Physics*, 48(1), pp. 120-132. doi:10.1134/S0001433812010021

21. Kallos, G., Nickovic, S., Papadopoulos, A., Jovic, D., Kakaliagou, O., Misirlis, N., Boukas, L., Mimikou, N., Sakellaridis, G. and Papageorgiou, J., 1997. The Regional Weather Forecasting System SKIRON: An Overview. In: G. B. Kallos, V. Kotroni and K. Lagouvardos, eds., 1997. *Proceedings of the Symposium on Regional Weather Prediction on Parallel Computer Environments (Athens, 15–17 October 1997)*. Athens, Greece: University of Athens, pp. 109-122.

22. Ivanov, V.A. and Belokopytov, V.N., 2013. *Oceanography of the Black Sea*. Sevastopol: MHI, 210 p.

23. Mamayev, O.I., ed., 1975. *Temperature – Salinity Analysis of World Ocean Waters*. Amsterdam: Elsevier, 374 p. doi:10.1016/s0422-9894(08)x7055-2

24. Oort, A.H., Ascher, S.C., Levitus, S. and Peixóto, J.P., 1989. New Estimates of the Available Potential Energy in the World Ocean. *Journal of Geophysical Research: Oceans*, 94(C3), pp. 3187-3200. doi:10.1029/JC094iC03p03187

25. Kubryakov, A.A., Bagaev, A.V., Stanichny, S.V. and Belokopytov, V.N., 2018. Thermohaline Structure, Transport and Evolution of the Black Sea Eddies from Hydrological and Satellite Data. *Progress in Oceanography*, 167, pp. 44-63. doi:10.1016/j.pocean.2018.07.007

About the authors:

Sergey G. Demyshev, Chief Research Associate, Head of Wave Theory Department, Marine Hydrophysical Institute of RAS (2 Kapitanskaya Str., Sevastopol, 299011, Russian Federation), Dr.Sci. (Phys.-Math.), **SPIN-code: 1848-2350, ORCID ID: 0000-0002-5405-2282, ResearcherID: C-1729-2016, Scopus Author ID: 57862712800**, demyshev@gmail.com

Ol'ga A. Dymova, Senior Research Associate, Marine Hydrophysical Institute of RAS (2 Kapitanskaya Str., Sevastopol, 299011, Russian Federation), Ph.D. (Phys.-Math.), **SPIN-code: 7565-1082, ORCID ID: 0000-0003-4036-2447, ResearcherID: P-9669-2015**, olgadym@yahoo.com

Nadezhda A. Miklashevskaya, Junior Research Associate, Marine Hydrophysical Institute of RAS (2 Kapitanskaya Str., Sevastopol, 299011, Russian Federation), **SPIN-code: 8476-2604, ORCID ID: 0000-0003-2619-343X, ResearcherID: P-2167-2017**, nmikl@rambler.ru

Contribution of the co-authors:

Sergey G. Demyshev – general scientific direction of the research; formulation of the study goals and objectives; discussion of the work results; mathematical model development; editing and supplementing the text of the paper; critical analysis and revision of the text

Ol'ga A. Dymova – review of literature on the research problem; exploring the concept; designation of the methodological basis of the study; carrying out calculations; processing and description of research results; analysis of the results and their interpretation; preparation of the paper text; data visualization / presentation in text

Nadezhda A. Miklashevskaya – processing and description of the results of the study; qualitative and quantitative analysis of the results; critical analysis and revision of the text

The authors have read and approved the final manuscript.
The authors declare that they have no conflict of interest.